Astronomy
&
Astrophysics

On the widths and ratios of Mg X 609.79 and 624.94 Å lines in polar off-limb regions

E. O'Shea[1], D. Banerjee[2], and J. G. Doyle[1]

[1] Armagh Observatory, College Hill, Armagh BT61 9DG, N. Ireland
    e-mail: [eos;jgd]@arm.ac.uk
[2] Indian Institute of Astrophysics, II Block, Koramangala, Bangalore 560 034, India
    e-mail: dipu@iiap.res.in

Abstract. Using measurements of Mg X 609.78 and 624.94 Å lines from the Coronal Diagnostic Spectrometer (CDS) on board SOHO, we seek to examine the variation of line width and line ratio in regions far off-limb at the Northern pole of the Sun. It is found that above $\approx 1150''$ the ratio of the two coronal Mg X resonance lines reduces to values that might be expected for a more radiatively dominant excitation mode. A comparison of the line widths with these ratios indicates that the line widths start to show a decrease in their values at the location where the dominant excitation changes from being collisionally to radiatively dominant, that is, at $\approx 1150''$. We suggest that the decrease in the line widths above $\approx 1150''$ is likely to be due to a reduction in the non-thermal component of the line widths caused by a damping of upwardly propagating Alfvén waves.

Key words. Sun: UV radiation – Sun: corona – Sun: atmosphere

1. Introduction

Two recent papers, e.g., Harrison et al. (2002) and O'Shea et al. (2003), have found evidence for line width decreases off-limb in the equatorial and polar regions, respectively. These line width decreases are taken as evidence for magnetic wave dissipation and, hence, heating of the corona. However, other papers, notably Wilhelm et al. (2004), have found no evidence for a narrowing of line widths in either the equatorial or polar regions. Using CDS data we investigate the variation of line widths off-limb in the Northern polar region of the Sun. For these observations we use the Mg X lines at 609.79 and 624.94 Å, two resonance lines from the lithium isoelectronic sequence. For lines belonging to the lithium isoelectronic sequence the relative intensities of the collisonally and radiatively excited components can be determined from a ratio of the doublet resonance lines. For the Mg X 624.94/609.79 ratio a value of 1:2 (0.5) will indicate a predominantly collisionally excited emission while a value of 1:4 (0.25) will indicate a predominantly radiatively excited emission (Kohl & Withbroe 1982). Using measurements of Mg X 609.79 and 624.94 Å lines, we seek to find evidence of line widths decreases far off-limb and to relate this to information provided by the Mg X ratios.

2. Observations and data reduction

2.1. Initial calibration and line fitting

For these observations we have used the normal incidence spectrometer (NIS), which is one of the components of the

Table 1. A log of the datasets obtained using the $4 \times 240''$ CDS slit in December 2002.

Date	Dataset	Pointing (X, Y)	Start/ End (UTC)	Exp. time (s)
17/12	SER150W:26478	59, 1071	18:03	60
17/12	SER75W:26479	60, 1213	20:54	120
27/12	SER150W:26542	0, 1070	18:10	60
27/12	SER75W:26543	−1, 1215	21:01	120

Coronal Diagnostic Spectrometer (CDS) on board the Solar and Heliospheric Observatory (SOHO), see Harrison et al. (1995). The details of the observations, including pointing and start times are summarised in Table 1. The data were obtained in a polar region during a period when the coronal holes at the poles were ill-defined. For the SER150W temporal series sequences the CDS slit was pointed in the North polar region in such a way that the bottom few pixels corresponded to the limb. For the SER75W sequences, the slit was shifted north to cover far off-limb regions, a sizable overlap of $\approx 100''$ being maintained between the SER150W and SER75W datasets. Using these two complementary sequences data was obtained for the coronal lines Mg X 609.79 and Mg X 624.94 Å ($\approx 1.25 \times 10^6$ K). Note that we shall henceforth refer to the lines without the following decimal places, e.g., 624 in place of 624.94, etc. The data was reduced using the most recent versions of the standard CDS routines (see http://solg2.bnsc.rl.ac.uk/software/uguide/

uguide.shtml) Before fitting the lines with a single Gaussian, and in order to increase the signal-to-noise ratio, we binned by 2 along the 143 pixel long slit to produce 70 pixels (4″ × 3.36″) in Y for the SER150W sequences, and by 4 to produce 35 pixels (4″ × 6.72″) in Y for the SER75W sequences. We then also summed in time over the 150 time frames in SER150W and the 75 time frames in SER75W to produce the required high signal-to-noise line profiles along the Y slit direction.

Harrison et al. (2002) discuss the relative contributions expected in the line width of an observed CDS line; the instrumental width, the thermal width and the non-thermal width. For CDS the instrumental width dominates but is an uncertain quantity due to CDS being designed to measure and compare line intensities rather than line profiles. Harrison et al. (2002) estimate it to have a full width half maximum (*FWHM*) value of ≈0.28 Å (≈0.17 Å in Doppler widths) for a Mg x 624 line obtained using the 4″ wide slit. More recently, Wilhelm et al. (2005) present estimates of CDS and SUMER line widths measured in off-limb regions. From the width measurements of Si xii 520 in their Fig. 4 it is possible to establish a maximum upper bound value for the CDS instrumental width of ≈0.29 Å. We suggest that the "real" instrumental width of the CDS instrument is somewhat below this upper bound value but larger than the value of ≈0.17 Å estimated by Harrison et al. (2002). However, as there are no SUMER measurements for the Si xii 520 line it is not possible to accurately deduce the CDS instrumental width by direct comparison with SUMER data. We shall therefore use the upper bound value from Si xii 520 (<0.29 Å) as our estimate of the CDS instrumental width in this letter. We note that the Mg x 624 line as measured by CDS is not useful for estimating instrumental width values due to its blends with a Si x line at 624.78 Å and a O iv line at 625.13 Å. These blends on the blue and red wings of the Mg x line have the effect of increasing the overall measured line width while only being responsible for, at maximum, 10% of the radiance of the blend (see, e.g., Wilhelm et al. 2004).

The values that will be quoted by us in this paper will be Doppler widths, i.e., half 1/e widths. As the CDS instrumental and thermal width are unchanging components, we can state that any change in the width of a CDS spectral line must be due solely to changes in its non-thermal component.

2.2. Scattered light

Often scattered light contributions are significant while making observations off-limb. As reported in Young et al. (1999), scattering within the NIS/CDS instrument can occur at two locations: (i) within the spectrograph; and (ii) within the telescope section. Type (i) scattering can be neglected as it is considered to take place only in the wavelength dispersion direction and not in the spatial direction. Evidence for this comes from the fact that the images obtained in NIS lines do not extend beyond the limits imposed by the slit size. The extent of type (ii) scattering has been discussed by David et al. (1997). Using pre-launch measurements of the point spread function (PSF) of the
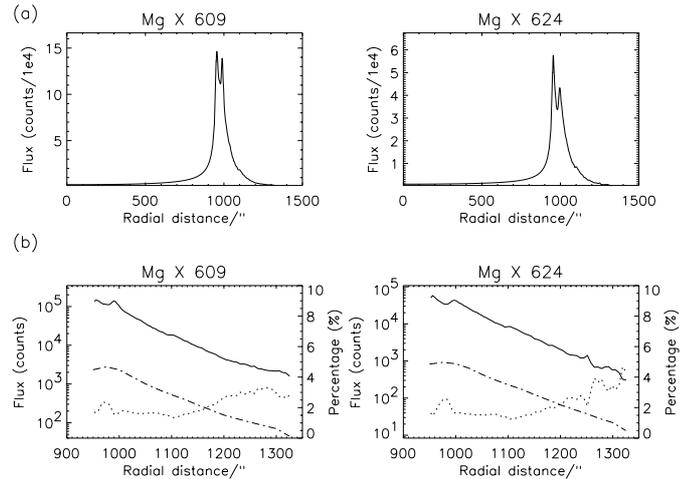

Fig. 1. a) Variation of total radiant flux as a function of radial distance from Sun centre, i.e., radial brightness profiles **b)** measured radiant flux off-limb (solid line), calculated flux due to scattering (dot-dash line) and the percentage of the total radiant flux due to scattering (dotted line).

CDS telescope at 68 Å, and extrapolating to the observed wavelengths in CDS GIS/NIS, together with a model of the solar brightness distribution, David et al. (1997) show that it is possible to estimate the proportion of the scattered light in the radiance measurements. The program CAL_CDS_STRAYLIGHT, available in the SSWIDL software tree, performs the necessary calculations. In Fig. 1a we show, up to 1325″, the solar brightness distributions used as the "model" in our calculations, that is, the variation of the flux as a function of radial distance from Sun centre. For locations belows ≈950″, where we lacked observational data, we used an approximate value for the radial flux distribution calculated from the $1/\cos\theta$ function, where θ is the angle between the viewing direction and a perpendicular line normal to the surface. These distributions conform to the brightness profile (c) discussed in David et al. (1997), i.e., emission from an isothermal corona with an exponential decrease of density with height. The values of flux above ≈1090″, where we used the data from the SER75W sequence, have been divided by 2 so that they match those of the lower SER150W sequence. In Fig. 1b we show the results of our calculations. For the coronal lines of Mg x 609 and 624 it can be seen that at no point does the scattering account for more than ≈4% of the total radiance and, thus, we feel that it can be discounted as a factor in the analysis of these lines.

3. Results

In Fig. 2 we plot the results of line width measurements for the December 17 and 27 datasets. These plots combine the results from the SER150W and SER75W datasets obtained on the same day and, taking the CDS pointing uncertainty of ≈3″ into account, at the same pointing locations (see Table 1). The data from the lower level SER150W observations are plotted up to an altitude of ≈1110″ and from there the data is from the higher level SER75W observations; something reflected in the lower number of data-points present from that point on.
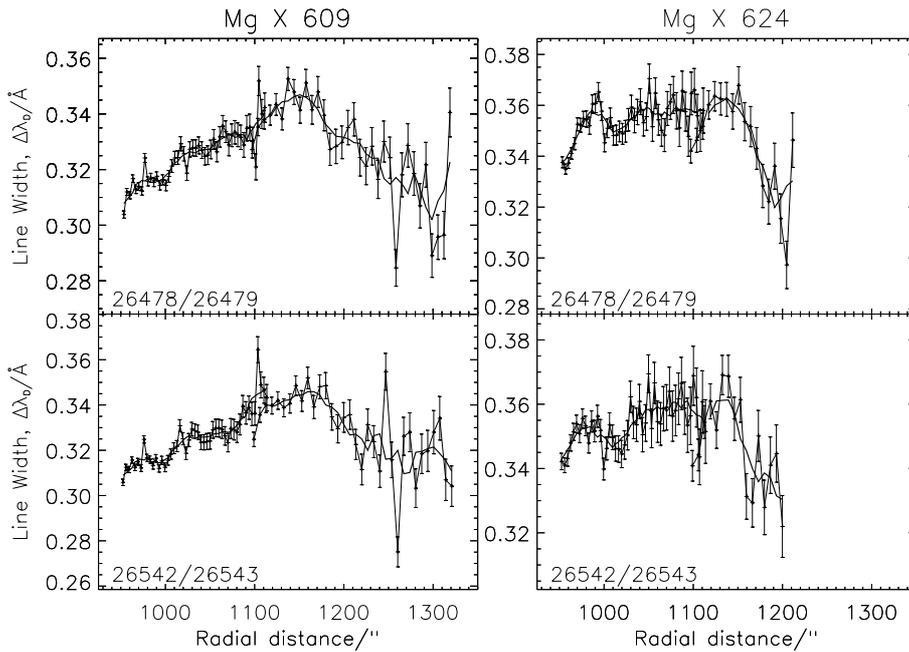
Fig. 2. Variation of the Doppler width (uncorrected for instrumental width contributions) versus radial distance for the 26 478/26 479 and 26 542/26 543 datasets, as indicated by the numbers shown in each plot. The thick black lines show the result of a box-car averaging to remove the effects of the FPN. Radial distance locations where the radiance fell below a critical S/N value do not show the results of the line width measurements.

There is a small overlap of 5 data-points allowed between the observations from the two datasets. Note that for some of the datasets in Fig. 2, and, in particular, for the Mg x 624 line, the line widths are not plotted at higher altitudes due to the low values of radiance at these greater heights. We chose not to plot any line widths from summed profiles that had a measured flux of less than a lower limit of ≈2500 counts, i.e. a S/N of ≈4. Gaussians with these S/N are still recognizable as such and so we chose this as a lower limit. It will be noticed that the results from Mg x 609 and 624 lines, although formed from the same ion and at the same temperature, show significant differences in line width. That is, the Mg x 624 line shows consistently larger values. This may be due to the effect of the blends of Si x at 624.78 Å and O iv at 625.13 Å in the Mg x 624 line, which have the result of increasing the overall measured line width.

Before discussing the line widths in Fig. 2 in more detail, we firstly draw the reader's attention to the fact that the two plots for Mg x 609 share many small-scale line width variations, e.g., between 1100 and 1200″ and, more obviously, between 1240 and 1270″. These small-scale variations are not caused by real physical effects but are due to an instrumental effect called "Fixed Patterning Noise" (FPN) which is found in the CDS slit in the North-South, i.e., along the slit, direction. This fixed-patterning is constant in time and is present in radiance, line-of-sight velocity and line-width maps of CDS data (C.D. Pike, 2004, private communication). This FPN generally causes small-scale variations in the line width values at the 3% level. We further note that there is another more general line width variation of about 5–6% from South to North along the slit due to variations in the scan mirror position. This more general effect is not constant in time and different datasets can show significant differences in the size of the effect. In order to reduce the effect of FPN on the data we perform a box-car averaging smoothing of 7 pixels (≈24″) along the slit for the SER150W datasets and a smoothing of 5 pixels (≈34″) along

the slit for the SER75W datasets. The results for this are shown as the over-plotted thick line in each of the plots.

For the Mg x 609 line of SUMER, Doschek et al. (2001) found line widths of 0.09–0.11 Å (0.15–0.18 Å, *FWHM*) between heights equivalent to 995″ and 1095″. For the Mg x 609 line in Fig. 2 we find widths of ≈0.315–0.335 Å between the same heights. Subtracting out the approximate CDS instrumental width of 0.29 Å (see Sect. 2.1) by a subtraction of squares, we can get a rough estimate of ≈0.12–0.17 Å for the actual width of the Mg x 609 line. Taking into account that the assumed instrumental width value of 0.29 Å is an upper bound value suggests that the "real" width of the Mg x 609 line between these heights is somewhat greater. However, the small difference between these values and those of Doschek et al. suggests that our results are fairly consistent with previous Mg x line width measurements.

In Fig. 2, it is possible to see that the line widths of both the Mg x lines increase up to an altitude of ≈1150″ before showing a general decrease above this height. As it is known that, for Alfvén waves, the energy flux is proportional to line width (Doyle et al. 1998) the question we must ask is: are the decreases in the line widths at the higher altitudes above 1150″ due to some form of wave dissipation? To examine this, we plot in Fig. 3 the ratio of the two Mg x lines versus height above the limb for each of the datasets. The values from the SER150W sequence are plotted up to a height of ≈1110″ and after that the values come from the SER75W sequence, with an overlap of ≈15″. These ratios have also been smoothed to remove the effects of the FPN discussed earlier. Just above the limb (>1000″) in Fig. 3, the ratio of the two Mg x lines have values that we would expect for a more collisionally dominant excitation mode, that is, values close to 0.5. There is a change, however, in the ratios at ≈1150″ where they begin a decrease to values more expected for radiatively dominant excitation, i.e.,
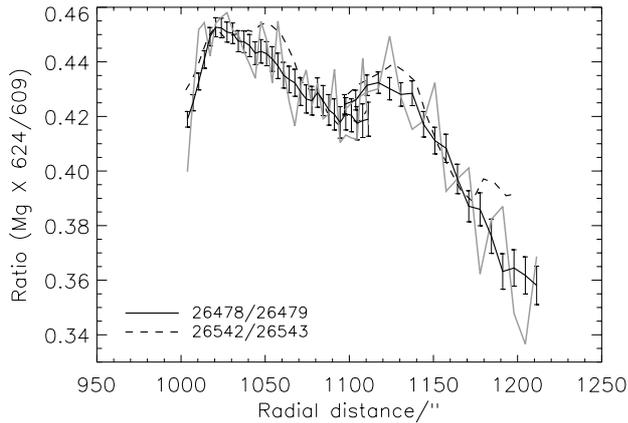
Fig. 3. Ratio of Mg X 624/609 as a function of radial distance in arcsec for the 26 478/26 479 and 26 542/26 543 datasets. Representative uncertainties for the 26 478/26 479 datasets are plotted as error bars. The original unsmoothed ratio values for the 26 478/26 479 datasets are shown in grey for comparison.

down towards values of 0.25. Similar results have been found previously by Singh (1985) for Fe X lines.

Note that between ≈1000 and 1020″ the Mg X ratios show an initial increase, before reaching maximum values of ≈0.45. This initial increase can be largely explained by blends of O III (609.70 Å) and O IV (609.83 Å) with the Mg X 609 line. These lower temperature lines can account for as much as 15% of the total radiance of the blend (Wilhelm et al. 2004) at locations close to the limb. At higher altitudes off-limb, the proportion of O III and O IV in the blend drops and the ratios return to their expected values of close to 0.5. The blending of the Mg X 624 line mentioned previously can also be expected to further complicate and alter the expected ratio values of 0.5 at these heights.

If we compare the ratios in Fig. 3 with the line widths in Fig. 2, it is clear that there is a large decrease in the line width and ratio values at almost exactly the same location, i.e., at ≈1150″. The decrease in the line ratios at this location suggests that the dominant excitation changes from being collisionally to radiatively dominant. The fact that the decrease in line widths occurs at approximately the same location as the decrease in the Mg X ratios suggests that the reduction in the nonthermal velocities may be linked in some way to this change in the dominant excitation, perhaps due to changes (decreases) in the electron density. We note that Hassler et al. (1990) found a plateau in their observed line widths between 1.1 and 1.2 $R_\odot$, which they considered might be due to either wave reflection and/or damping in the lower corona. In our observations, up to ≈1.35 $R_\odot$, and, so, further out than those of Hassler et al., we find a definite decrease in the line width values above ≈1.2 $R_\odot$, i.e., ≈1150″. The fact that we see a reduction in the line widths would suggest that what we are seeing in these data is a damping of the waves assumed to be responsible for the initial increase in the line widths off-limb.

4. Conclusions

We find evidence for a decrease in line widths at a certain height above the limb in polar regions. The decrease in line width above 1150″ coincides with the location where the observed line ratio of Mg X 624/609 indicates a change from a collisionally to a radiatively dominant excitation regime. Banerjee et al. (1998) and Doyle et al. (1998) have shown that the non-thermal velocity above a polar coronal hole, as measured from the Si VIII line in SUMER spectra, shows a deviation from a linear increase above 200″, and indicated a region of plateau. We suggest that the decrease in line widths above ≈1150″ is caused by damping of upwardly propagating MHD waves. Pekünlü et al. (2002) investigated Alfvén wave propagation in the linear incompressible MHD context. They show that Alfvén waves propagating along magnetic flux tube go through refraction and get damped via viscous dissipation and resistivity. The radial profile of their energy flux density (Fig. 4) shows an initial rise up to 1.15 $R_\odot$, where it peaks and further on declines less steeply than the rising phase. Thus, this theoretical work supports our observational evidence of damping of upwardly propagating waves. Finally, we note that most of the density diagnostics calculations using theoretical line ratios only take collisional excitation into consideration. The result presented here suggest that line ratio calculations of electron densities, using solely collision excitation calculations, may be incorrect in regions far off-limb where radiative excitation becomes stronger than collisional excitation (≥1150″).

References

Banerjee, D., Teriaca, L., Doyle, J. G., & Wilhelm, K. 1998, A&A, 339, 208
David, C., Gabriel, A. H., & Bely-Dubau, F. 1997, Proc. 5th SOHO Workshop, ESA SP-404, 313
Doschek, G. A., Feldman, U., Laming, J. M., Schühle, G. A., & Wilhelm, K. 2001, ApJ, 546, 559
Doyle, J. G., Banerjee, D., & Perez, M. E. 1998, Sol. Phys., 181, 91
Doyle, J. G., Teriaca, L., & Banerjee, D. 1999, A&A, 349, 956
Harrison, R. A., Sawyer, E. C., Carter, M. K., et al. 1995, Sol. Phys., 162, 233
Harrison, R. A., Hood, A. W., & Pike, C. D. 2002, A&A, 392, 319
Hassler, D. M., Rottman, G. J., Shoub, E. C., & Holzer, T. E. 1990, ApJ, 348, L77
Kohl, J. L., & Withbroe, G. L. 1982, ApJ, 256, 263
O'Shea, E., Banerjee, D., & Poedts, S. 2003, A&A, 400, 1065
Pekünlü, E. R., Bozkurt, Z., Afsar, M., Soydugan, E., & Soydugan, F. 2002, MNRAS, 336, 1195
Singh, J. 1985, Sol. Phys., 95, 253
Wilhelm, K., Dwivedi, B. N., & Teriaca, L. 2004, A&A, 415, 1133
Wilhelm, K., Fludra, A., Teriaca, L., et al. 2005, A&A, in press
Young, P. R., Klimchuk, J. A., & Mason, H. E. 1999, A&A, 350, 286